Biophysical Chemistry 193–194 (2014) 20–26

Contents lists available at ScienceDirect

Biophysical Chemistry

journal homepage: http://www.elsevier.com/locate/biophyschem

Effect of urea and trimethylamine *N*-oxide on the binding between actin molecules

Kuniyuki Hatori *, Takuya Iwasaki, Reito Wada

Department of Bio-Systems Engineering, Graduate School of Science and Engineering, Yamagata University, Yonezawa 992-8510, Japan

HIGHLIGHTS

- Urea and TMAO decreased the end-to-end annealing rate constant of actin filaments.
- Only TMAO enhanced the thermal stability and polymerization rate of actin monomers.
- The deleterious effect of urea on polymerization was completely offset by TMAO.

GRAPHICAL ABSTRACT

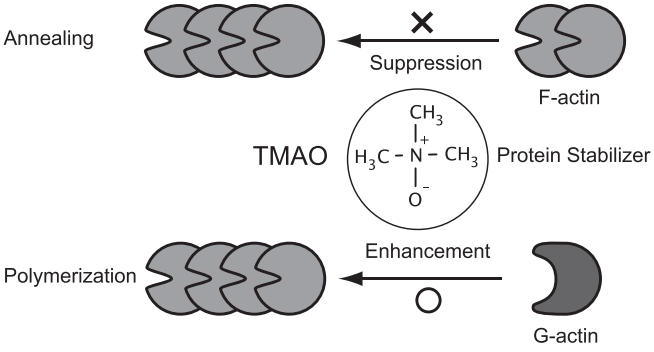

ARTICLE INFO

Article history:
Received 12 June 2014
Received in revised form 14 July 2014
Accepted 14 July 2014
Available online 23 July 2014

Keywords:
Denaturant
Protein stabilizer
Muscular protein
Polymerization
End-to-end annealing
Protein–protein interaction

ABSTRACT

Urea and trimethylamine *N*-oxide (TMAO) are known to denature and stabilize proteins, respectively. We examined two actin-binding processes, namely, end-to-end annealing of actin filaments (F-form) and the polymerization of actin monomers (G-form) into filaments, in the presence of urea, TMAO, and both solutes. Fluorescence microscopy for direct observation of actin filaments bound by fluorescent phalloidin revealed that the annealing rate constant decreased as the concentrations of urea or TMAO increased. Fluorescence spectroscopy with pyrene-labeled actin monomers showed that urea decreased the polymerization rate, whereas TMAO enhanced the rate. The decrease in the polymerization rate constant and thermal stability induced by 0.6 M urea was almost completely ameliorated by the addition of 0.3 M TMAO. These results suggest that TMAO-dependent stabilization of actin structure facilitates the binding of G-form actin to the ends of F-form actin filaments. Conversely, the binding between ends of mature filaments was impaired by TMAO.

1. Introduction

Actin polymerization processes have been intensely studied because the morphology and dynamics of actin filaments are crucial for cell motility [1–3]. In *in vitro* experiments, actin monomers (G-form actin) spontaneously polymerize into filaments (F-form actin) when salt and magnesium ions are added to the actin solution. When G-form actin monomers associate with the ends of F-form actin filaments, they undergo conformational changes that are marked by a rotation between sub-domains [4–6]. It is likely that this structural change strengthens intermolecular interactions of actin constituents within filaments and enhances the stability of the filament structure [5]. These observations raise the issue of how stabilization of the actin structure contributes to the association between actin molecules.

Abbreviations: TMAO, trimethylamine N-oxide; ATP, adenosine-5′-triphosphate; TMR, tetramethyl-rhodamine; HMM, heavy meromyosin; NEM, *N*-ethylmaleimide; CD, circular dichroism; DTT, dithiothreitol.

* Corresponding author. Tel./fax: +81 238 26 3727.
E-mail address: khatori@yz.yamagata-u.ac.jp (K. Hatori).

http://dx.doi.org/10.1016/j.bpc.2014.07.001
0301-4622/

To evaluate protein structure and function, investigators generally study protein unfolding and de-stabilization in the presence of denaturants or under various physical conditions [7–14]. In particular, urea and guanidine chloride are widely employed as protein denaturants. High concentrations of urea likely induce protein unfolding *via* the exposure of hydrophobic regions to an aqueous environment through solvation of the peptide backbone and side chains [7–9]. In contrast, trimethylamine-*N*-oxide (TMAO), a natural osmolyte found in water-stressed organisms [15], can act as a protein stabilizer and chemical chaperone [16–28]. The exclusion of TMAO solutes from protein surfaces through unfavorable interactions with the protein backbone tends to thermodynamically favor a folded (rather than extended) protein structure, which is suggested to underlie the stabilizing effects of TMAO [12,16–18]. However, it was proposed that TMAO can also interact with proteins [19] and modulate hydrogen bonds between water and proteins [20,21], and a consensus for TMAO-dependent protein stabilization has not yet been reached.

Although many studies on the effect of urea and TMAO on proteins have focused on the structural stability and folding/unfolding processes of proteins, little information is available regarding their effect on protein–protein interactions [29–31]. Our previous work revealed that TMAO suppresses the motility of actin filaments that interact with heavy meromyosin (HMM) molecules, even though the HMM structure is stabilized [31]. In addition, the deleterious effect of 0.6 M urea on motility was offset by the presence of TMAO at 0.3 M, a concentration that is within the physiological upper limits (386 mmol/kg) of a deep sea-dwelling organism [32]. In addition to physiological significance of urea and TMAO, to understand the biophysical role of these osmolytes, we here extended our studies of actin–myosin interactions to demonstrate that TMAO has differential effects on the binding between molecules composed of the G- and F-forms of actin.

2. Materials and methods

2.1. Chemicals and proteins

Urea and TMAO were purchased from Nacalai Tesque (Kyoto) and MP Biomedicals (California), respectively. Tetramethylrhodamine–phalloidin (TMR–phalloidin) was purchased from Sigma-Aldrich (St. Louis, MO). All chemicals were of special grade and were used without further purification. Actin monomers (G-actin) were purified from rabbit skeletal muscles according to the method of Spudich and Watt [33] and were stored at 4 mg/mL in G-buffer (2 mM Tris–HCl (pH 8.0), 0.2 mM ATP, 0.1 mM $CaCl_2$, 0.02% 2-mercaptoethanol, 0.05% NaN_3) at 4 °C. Purified actin monomers were used within 2 weeks.

2.2. Measurement of actin filament length for estimation of the annealing rate constant

The length of the actin filaments was measured by fluorescence microscopy. Initially, actin filaments (0.1 mg/mL) were fluorescently labeled and stabilized by TMR–phalloidin in a standard solution (25 mM KCl, 25 mM imidazole-HCl (pH 7.4), 2 mM $MgCl_2$, 1 mM ATP, and 1 mM DTT). The sample was incubated for 2 days at 4 °C. Subsequently, the prepared sample (50 μL) was added to 450 μL of the standard solution containing urea and/or TMAO, and the mixture was immediately sonicated using an ultrasonic homogenizer to make short filaments (<1 μm). The sonicated sample was incubated at 25 °C, at which point annealing was initiated. The annealing was performed in the presence of 1 mM ATP. At 10 min intervals, 10 μL aliquots were taken from the specimen and added to 990 μL of the standard solution containing oxygen scavengers (3 mg/mL glucose, 0.02 mg/mL catalase, and 0.12 mg/mL glucose oxidase) because the annealing reaction was terminated by dilution. Immediately, 10 μL of diluted sample was dropped on a poly-lysine-coated thin slide glass (No. 1, 24 × 50 mm, Matsunami, Japan) and was observed under a fluorescence microscope (objective TIRF 100× H; Ti–U, Nikon, Japan). Fluorescence images were taken with an EM-CCD camera (DE-500, Hitachi Kokusai, Japan). The lengths of 100 individual filaments at each time point were measured using ImageJ software (Rasband, W.S., ImageJ; National Institutes of Health, Bethesda, Maryland, USA). The length was obtained in terms of actin units based on an estimated value of 389 actin subunits/μm. To determine the annealing rate constant, data from the time course were fitted to the equation derived by Andrianantoandro et al. [34]:

$$-dN/dt = k_a N^2/L, \tag{1}$$

where N is the concentration of filaments, dN/dt is the annealing rate, k_a is the annealing rate constant per subunit length, and L is the mean length of actin filaments in subunits. Using P as the initial actin concentration (0.24 μM), N = P / L was substituted into Eq. (1). Solving this differential equation, we obtained the relationship between length and time (t) as follows:

$$L^2 = 2k_a Pt + {L_0}^2, \tag{2}$$

where L_o is the initial filament length.

2.3. Fluorescent measurement of pyrene-labeled actin monomer polymerization

Actin monomers were labeled with N-(1-pyrenyl)iodoacetamide according to the method of Kouyama and Mihashi [35]. To start the polymerization, 100 μL of actin monomers containing 8% pyrene-labeled actin (1 mg/mL) were added to 400 μL of polymerization buffer (final concentrations in 500 μL: 25 mM KCl, 25 mM HEPES (pH 7.4), 1 mM ATP, 2 mM $MgCl_2$, and 0.5 mM DTT, with various concentrations of urea and TMAO). Immediately, 500 μL of the sample was infused into a cuvette (optical path for excitation, 0.2 cm; optical path for emission 1.0 cm), and then the fluorescent intensity was monitored using a fluorescence spectrometer (F-2500, Hitachi, Japan) at 25 °C. Excitation was set at 365 nm (band pass 2.5 nm), and emission was set at 407 nm (band pass 5.0 nm). Development of intensity with time (except for data obtained during the clearing phase) was fitted into the equation for a simple polymerization model, which only considers the association with, or dissociation from, single filaments [1] as follows:

$$-dC/dt = k_{on} mC - k_{off} m, \tag{3}$$

where C is the concentration of actin monomers, and −dC/dt is the decrease rate of C. k_{on}, k_{off}, and m denote the polymerization rate constant, the dissociation rate constant, and the concentration of the actin filament terminals, respectively. Because the concentration of polymerized actin molecules (P) is equal to the difference between the total concentration (C_o) and concentration of actin monomer (C), Eq. (3) is transformed into the following equation:

$$P = C_o - k_{off}/k_{on} + (k_{off}/k_{on} - C_o)\exp(-k_{on} m t). \tag{4}$$

In this study, the concentration of filament terminals (m) was not determined, and we assumed that emission intensity was proportional to the concentration of polymerized pyrene-labeled actin. In this study, C_0 was set at 4.8 μM.

2.4. Observation of polymerization of actin monomers into filaments

Polymerization of actin monomers was directly observed under a fluorescent microscope according to the method of Ishiwata et al. [36]

with slight modifications. Specifically, we used NEM-modified HMM [37] with short actin filaments (acto-NEM-HMM) as the nucleus for growth rather than EDC-crosslinked acto-HMM. First, acto-NEM-HMM solution was prepared with 0.3 μg/mL TMR–phalloidin–actin and 2 μg/mL NEM-HMM in the standard solution (25 mM KCl, 25 mM imidazole-HCl (pH 7.4), 2 mM $MgCl_2$, 0.5% 2-mercaptoethanol). This sample was sonicated to obtain short filaments. To fix the acto-NEM-HMM to a glass surface, the sonicated sample was perfused into the flow cell constructed from a collodion-coated thin slide glass and a cover glass. Five minutes later, the unfixed acto-NEM-HMM in the flow cell was removed by perfusion with 10 mg/mL BSA in the standard solution. Actin monomers were added at 0.14 μM into the polymerization buffer (25 mM KCl, 10 mM imidazole-HCl (pH 7.4), 2 mM $MgCl_2$, 1 mM ATP, 0.1 μM TMR-phalloidin, 0.12 mg/mL glucose oxidase, 3 mg/mL glucose, 0.02 mg/mL catalase, and 0.5% 2-mercaptoethanol, with various concentrations of urea and TMAO). Immediately, this mixture was perfused into the flow cell, and the reaction was initiated. The gap in the flow cell was sealed with an enamel coating. The specimen was observed under a fluorescence microscope at 25 °C over a 1-h period.

2.5. Circular dichroism (CD) measurement of the thermal stability of actin monomers

CD spectra for actin monomers were recorded on a CD spectrometer equipped with a Peltier thermostated cuvette holder (J-820, Jasco, Japan). The solutions were examined under 5 mM HEPES (pH 7.4), 0.1 mM $CaCl_2$, 0.1 mM DTT, 0.01 mM ATP, and 0.05 mg/mL actin. The mean residue molar ellipticity was determined as the value at which the observed ellipticity was divided by both the optical pass length (0.5 cm) and the residue molar concentration (0.45 mM for 0.05 mg/mL actin). The thermal unfolding transition was monitored by measuring the ellipticity at 222 nm as a function of temperature in the range of 25–85 °C (heating rate: 2 °C/min). To determine T_m (midpoint of denaturation), the data were fitted into following:

$$\theta(T) = (\theta_N + \theta_D \exp(-(\Delta H_m/R)(1/T - 1/T_m)))/(1 + \exp(-(\Delta H_m/R)(1/T - 1/T_m))). \quad (5)$$

Here, θ and T are the ellipticity and absolute temperature, respectively. θ_N and θ_D are the ellipticities for the native and denaturant forms, respectively. ΔH_m and R are the enthalpy change and gas constant, respectively. In this study, ΔH_m was not evaluated because the unfolding of actin is irreversible with respect to temperature.

3. Results

3.1. Annealing of actin filaments in the presence of urea and TMAO

Actin filaments were stabilized and visualized by the binding of TMR–phalloidin. These filaments can bind each other *via* barbed and pointed ends, as described for the end-to-end annealing of actin filaments [34]. Fig. 1 shows images of TMR–phalloidin–actin filaments immediately and 20 min after fragmentation. Longer filaments were observed over time because of increased annealing. Filament lengths in the presence of urea or TMAO appeared shorter than those of controls. Fig. 2A demonstrates that mean filament length increased as the reaction proceeded. The annealing rate constant, estimated by fitting of the data into Eq. (2), decreased from 1.1 to 0.8 ($nM^{-1}\ s^{-1}$) as the concentration of TMAO increased over the range of 0–1.0 M (Fig. 2B). The addition of 0.1 M urea led to a 50% decrease in the rate constant, whereas the effect of TMAO was more modest. Furthermore, increasing the amount of TMAO up to 0.3 M partially abrogated the decrease in the rate constant caused by 0.6 M urea, with the value increasing from 0.5 to 0.65 ($nM^{-1}\ s^{-1}$) (Fig. 2C).

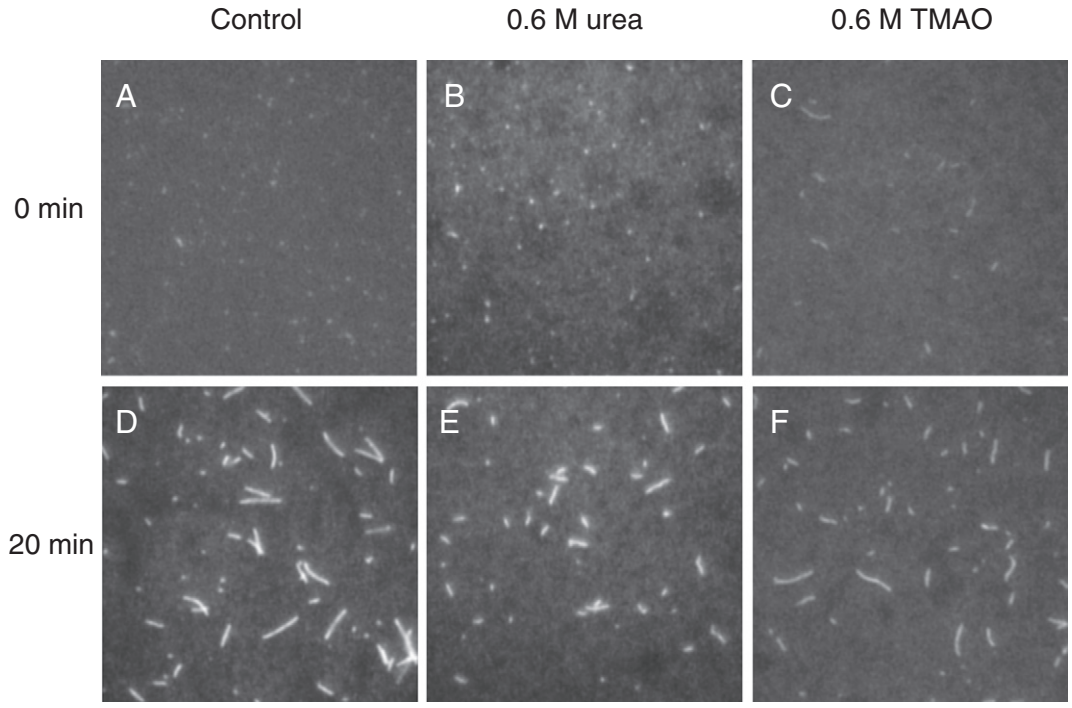

Fig. 1. Typical fluorescence images of TMR–phalloidin-bound actin filaments in the presence of urea or TMAO. The control without solutes is depicted in A, D. The presence of 0.6 M urea is shown in B and E and that of 0.6 M TMAO is shown in C and F. A, B, and C show images taken just after fragmentation. D, E, and F show images taken 20 min after fragmentation for preparations different from those in A, B, and C. The width and height of each image are both 30 μm.

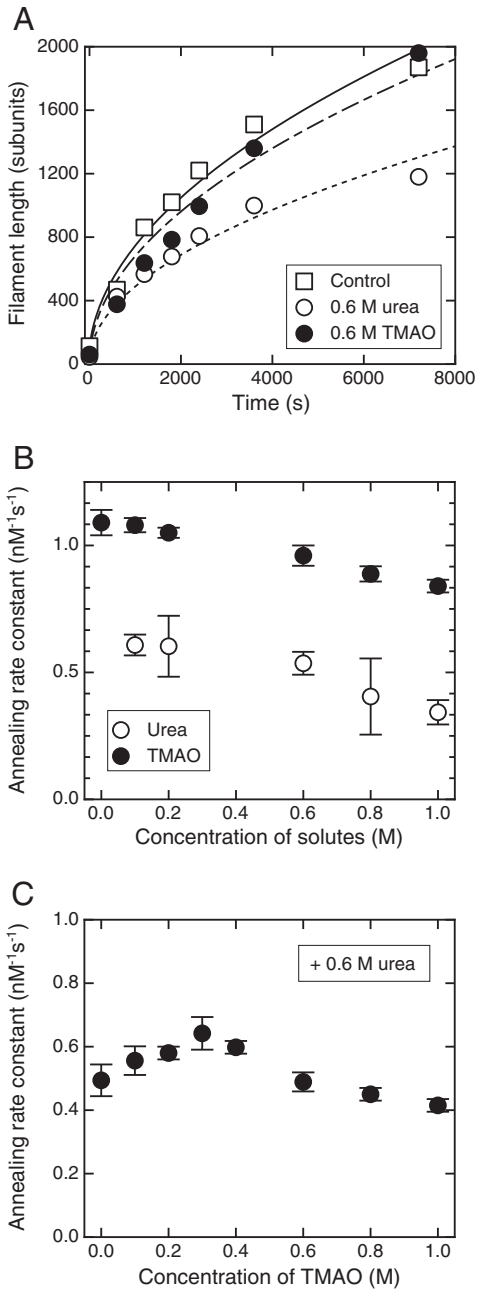

Fig. 2. Time courses of filament growth (A) and annealing rate constants (B, C) in the presence of urea, TMAO, and both solutes. A is the typical length change in the absence (open squares) and presence of 0.6 M urea (open circles) or 0.6 M TMAO (filled circles), and data were fitted to an irrational function to determine the annealing rate constant per unit length (see Section 2.2.). B and C show the dependence of annealing rate constants on the concentrations of urea (open circles) or TMAO (filled circles), and on the concentration of TMAO in the presence of 0.6 M urea, respectively. Error bars indicate the standard deviation estimated from 2 to 3 independent experiments performed under similar conditions.

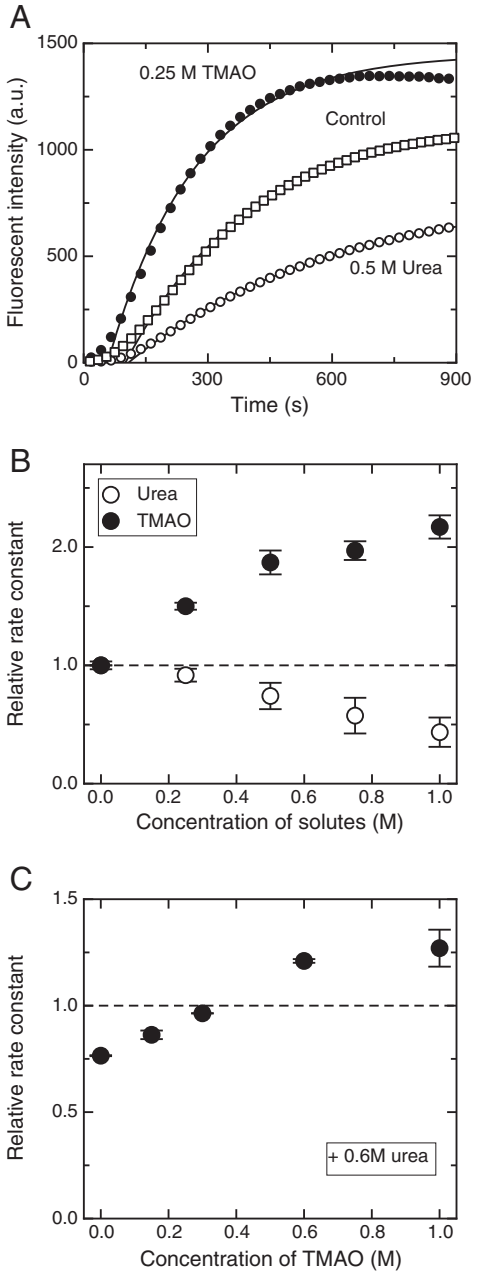

Fig. 3. Time courses of the development of the fluorescence of actin solutions with 8% pyrene-labeled actin (A) and relative polymerization rate constants (B, C) in the presence of urea, TMAO, and both solutes. A shows the typical fluorescent intensity changes in the absence (open squares) or presence of 0.6 M urea (open circles) and 0.6 M TMAO (filled circles), and the data were fitted to an exponential function to determine a parameter (k_{on} m) for the polymerization rate constant (see Section 2.3.). Because the absolute rate constant could not be determined in this study, each parameter was divided by that of the control, to yield a relative polymerization rate constant. B represents the dependence of the relative polymerization rate constant on the concentrations of urea (open circles) or TMAO (filled circles). C represents the TMAO concentration dependence of the relative polymerization rate constant in the presence of 0.6 M urea. Error bars indicate the standard deviation estimated from 2 to 3 independent experiments performed under similar conditions.

3.2. Polymerization of actin monomers in the presence of urea and TMAO

The polymerization of actin monomers with pyrene-labeled actin was monitored by fluorescence spectroscopy. Fig. 3A shows the time course of polymerization in the presence of urea or TMAO. The development of fluorescence was decreased by the addition of urea but was increased by the addition of TMAO. To compare the polymerization rate constants under various conditions, the time course was fitted into Eq. (4) to provide a simple model, in which only the association with and the dissociation from single filaments is considered. The kinetics of nucleus formation in the lag phase were not considered. In this study, because estimation of the number of nuclei was challenging, the absolute value of the rate constants could not be determined. Therefore, we evaluated the polymerization capacity as the relative rate constant compared with the control. The rate constant gradually decreased to 50% of the initial value as the urea concentration increased

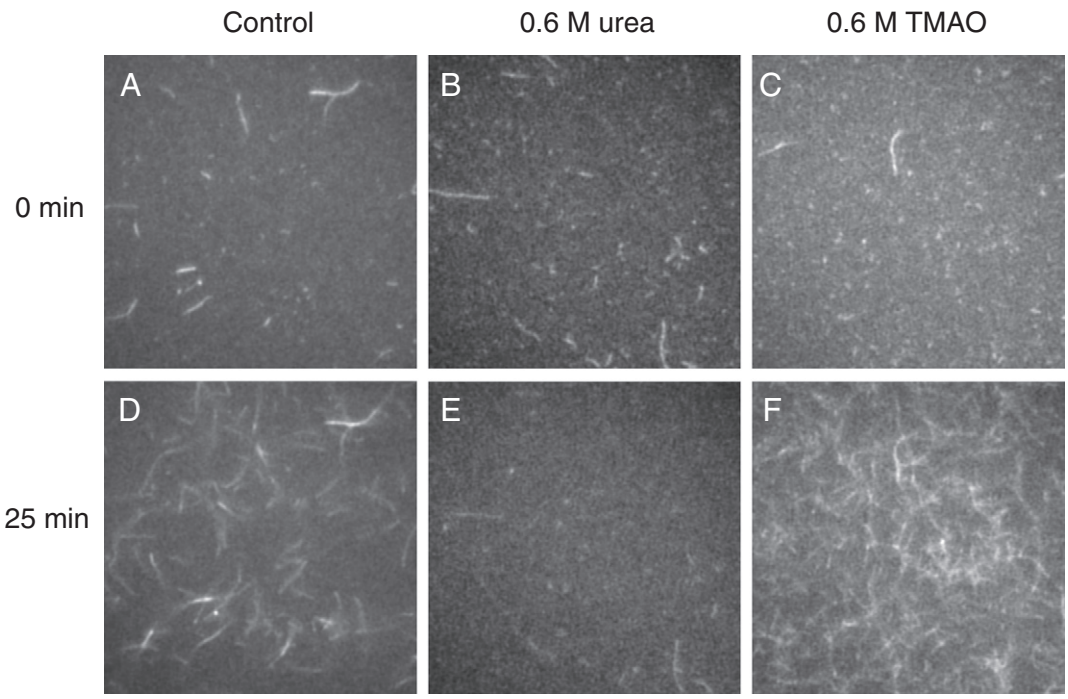

Fig. 4. Typical fluorescence images of actin polymerization in the presence of urea or TMAO. The control without solutes is depicted in A, D. The results with 0.6 M urea and 0.6 M TMAO are depicted in B, E and in C, F, respectively. A, B, and C show images taken just after initiation of polymerization in nuclei. D, E, and F show images taken 25 min after initiation of the reaction at the same location as in A, B, and C. The width and height of each image are both 30 μm.

from 0 to 1.0 M. In contrast, the addition of 1.0 M TMAO induced a two-fold increase in the rate constant (Fig. 3B). Furthermore, the urea-dependent decrease in the rate constant was gradually reversed as TMAO concentration increased, and was almost fully recovered by addition of 0.3 M TMAO (Fig. 3C). To confirm these observations, we also examined the polymerization of individual actin filaments using fluorescence microscopy. Actin filaments grew several micrometers over a 25 min period (Fig. 4D). In the presence of 0.6 M urea, there was no change in the filament length (Fig. 4E). In contrast, actin filaments in the presence of 0.6 M TMAO became longer than those in control samples, although the length of individual filaments could not be separately measured as they tended to overlap (Fig. 4F). The addition of 0.3 M TMAO restored the growth of filaments treated with 0.6 M urea (date not shown). Both the study with pyrene probes and direct observation indicated that TMAO enhanced the polymerization of actin monomers into the filaments.

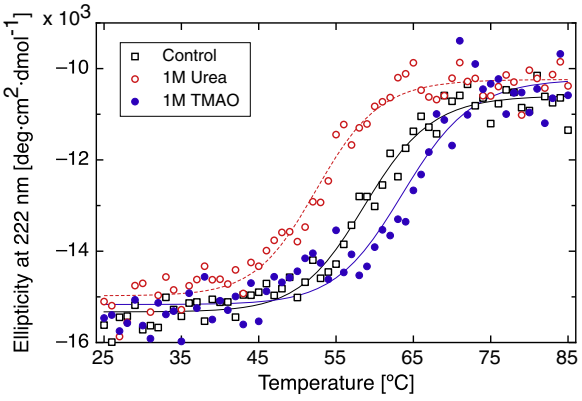

Fig. 5. Temperature dependence of the ellipticity of monomeric actin in the presence of urea or TMAO. Open squares, open circles, and filled circles indicate control without solutes and the presence of 1.0 M urea and 1.0 M TMAO, respectively. Data were fitted to Eq. (5) to determine the transition temperature (T_m) at the midpoint between the upper and the lower limits of observed ellipticity.

3.3. Thermal stability of actin monomers in the presence of urea and TMAO

The thermal stability of actin monomers was examined using CD spectroscopy as the temperature was raised to 85 °C. Fig. 5 shows the change of ellipticity at 222 nm with the increase in temperature, indicating a change in the proportion of alpha in the helices in solution. Using the lower and upper limits of the observed ellipticity to represent the contents of native and unfolding forms of actin, respectively, we estimated the transition temperature (T_m) at the midpoint of these limits to be 59 °C in the control. Urea and TMAO at 1.0 M changed the T_m to 53 °C and 64 °C, respectively, which indicates that urea decreases the structural stability of actin monomers, whereas TMAO increases their stability. In addition, in the presence of both 0.6 M urea and 0.3 M TMAO, the T_m was 56 °C.

4. Discussion

4.1. Comparison between annealing and polymerization of actin

Generally, TMAO at neutral pH stabilizes the structure of various proteins [28]. We also found that the structure of actin is stabilized by TMAO, as was previously observed in the case of heavy meromyosin molecules [31]. The stabilization may occur because TMAO tends to be excluded from protein surfaces, which results in a preferential native folding of proteins [16]. However, urea can destabilize the structure of actin and heavy meromyosin [31]. When urea interacts with the backbone and side chains of proteins, it causes the breakage of intrabackbone hydrogen bonds and eventually induces protein unfolding [7]. Our present study using actin as an example shows how such alterations of stability can affect protein–protein interactions.

End-to-end annealing of actin filaments was first demonstrated by Andrianantoandro et al. [34]. Similarly, we observed an increase in length as the result of end-to-end annealing. Unexpectedly, although

TMAO increased the stability of the actin structure, it inhibited end-to-end binding between phalloidin-stabilized filaments. We have previously reported that actin-activated ATPase activity and sliding velocity were significantly inhibited to a greater extent by TMAO than by urea [31,38]. Similarly, the dissociation rate constant of actin from HMM in the absence of ATP is also increased by the addition of TMAO. These results suggest that the interaction between actin filaments and HMM heads that occurs with conformational changes in HMM is inhibited by TMAO because of excessive stabilization. However, the present study shows that pre-stabilized actin filaments are also susceptible to TMAO-dependent inhibition of end-to-end binding. It is possible that temporary alterations at the ends of F-form actin filaments are necessary to favor docking of barbed and pointed ends for annealing. For instance, the D-loop in sub-domain 2 of actin changes shape in transition from the G- to the F-form [4–6]. Because the conformational change in an actin monomer is likely to occur after binding at the end of filaments [5], it may be difficult for the pointed end subjected to post-structural changes to suitably rebind to the barbed end once the F-form is further strengthened and stabilized. However, although the structure of capping protein-associated barbed ends has been determined [39], the structure of the free ends of actin filaments is still unknown. In the future, it will be essential to determine whether the structure of the free ends of filaments is similar to that of the F-form actin constituents that are incorporated into the filaments. Alternatively, TMAO may modify the filament structure itself, as it is possible that actin constituents within the filaments have multiple states [40]. In the absence of further structural information, we cannot determine the reason for the inhibition of the annealing.

Pyrene-labeled actin monomers are useful as a probe to monitor polymerization based on the increase in their fluorescent intensity with the transition from the G-form to the F-form [35]. Using this method, we clearly show that the rate constant is increased by TMAO but decreased by urea. For confirmation, we directly observed the growth of actin filaments, which also allowed us to directly estimate the polymerization rate constant [36]. The filament growth rate we report is in the same range as that in previous reports (approximately 80 nm/min at 0.14 μM actin) [36], although the clarity of the fluorescence images we took was insufficient to precisely measure the length of individual filaments. Together, the pyrene-labeled actin study and our direct observations demonstrate that TMAO facilitates the polymerization of actin monomers into filaments, whereas urea blocks polymerization. In the same manner, urea/TMAO caused variations in the stability of the actin structure. Structural studies suggest that during the transition between G- and F-forms, the outer domain of actin undergoes rotation perpendicular to the actin helix axis, or around 40° relative to the axis [4,5]. We suggest that TMAO may suppress such a conformational change in actin monomers by stabilizing their structure. This discrepancy between enhancing polymerization and suppression of structural changes may be explained as follows. During the first stage of polymerization, G-form actin preferentially binds to a filament end, and TMAO-induced stabilization of G-form actin facilitates this process. Subsequently, a bound actin monomer undergoes a conformational change because the F-form is more stable than the G-form in the context of a filament because of the intermolecular interaction between actin units. Thus, once actin monomers bind to the filaments, stabilization by TMAO can be helpful in the transition to the F-form.

4.2. Opposing effects of urea and TMAO on actin binding

TMAO can counteract the deleterious effects of urea on protein structure and is most effective when present in a 1:2 (TMAO:urea) molar ratio [13,23]. In addition, our previous study revealed that the counteractive effect of 0.6 M urea and 0.3 M TMAO likely occurs during the interaction of motile actin filaments with HMM molecules, although this counteraction was incomplete [31]. In contrast, actin-activated ATPase activity is not affected by the counteraction. Thus, the ability of TMAO to antagonize the effects of urea depends on the specific protein–protein interaction in question.

Here we also show that the addition of 0.3 M TMAO counteracted the reduction in annealing rate that was induced by 0.6 M urea, although treatment with either solute alone led to a reduction in the rate constant. However, the counteractive effect was only partial (an increase from 45% to 58% compared with the control). Therefore, direct interaction between urea and TMAO solutes alone cannot explain their counteraction during filament annealing. Urea was more effective in decreasing the annealing rate constant than TMAO. We suggest that urea solutes may preferentially bind to regions in filament ends, which are crucial for annealing, because the presence of TMAO has no effect on the interaction of urea with some proteins [41].

During polymerization, 0.3 M TMAO almost fully reversed the reduction in the polymerization rate constant that was induced by 0.6 M urea. Similarly, the thermal stability of actin molecules was enhanced by 0.3 M TMAO, which ameliorated the inhibition induced by 0.6 M urea (data not shown). Thus, both the polymerization and thermal stability were enhanced by the addition of TMAO, which had the opposite effect of the addition of urea. Moreover, the change in the polymerization rate induced by TMAO was twice that induced by urea, as shown in Fig. 3B. Thus, TMAO (positive effector) and urea (negative effector) act in an additive manner to facilitate the polymerization and stabilization of actin molecules.

5. Conclusion

Urea induced a decrease in both the annealing rate and polymerization rate of actin molecules. TMAO, which acts as a protein stabilizer, also decreased the annealing rate of actin filaments even though it pre-stabilized the F-form. In contrast, the polymerization of actin monomers, which is accompanied by their conformational change, was significantly enhanced by the presence of TMAO. The effect of TMAO on the incorporation of G-form actin monomers into the filaments was different from that on the end-to-end binding of F-form actin filaments. These results as well as the data from a further thermodynamic analysis of the effect of urea and TMAO on the sub-domains of proteins together provide insights into how protein stability and conformation affect protein–protein interactions.

Acknowledgments

We would like to thank Mr. N. Nomura and Mr. Y. Hosogoe of Yamagata University for their technical assistance.

References

[1] F. Oosawa, S. Asakura, Thermodynamics of the Polymerization of Protein, Academic press, London, 1975.
[2] A.E. Carlsson, Actin dynamics: from nanoscale to microscale, Annu. Rev. Biophys. 39 (2010) 91–110.
[3] R. Dominguez, K.C. Holmes, Actin structure and function, Annu. Rev. Biophys. 40 (2011) 169–186.
[4] T. Oda, M. Iwasa, T. Aihara, Y. Maéda, A. Narita, The nature of the globular- to fibrous-actin transition, Nature 457 (2009) 441–445.
[5] K. Murakami, T. Yasunaga, T.Q. Noguchi, Y. Gomibuchi, K.X. Ngo, T.Q. Uyeda, T. Wakabayashi, Structural basis for actin assembly, activation of ATP hydrolysis, and delayed phosphate release, Cell 143 (2010) 275–287.
[6] T. Fujii, A.H. Iwane, T. Yanagida, K. Namba, Direct visualization of secondary structures of F-actin by electron cryomicroscopy, Nature 467 (2010) 724–728.
[7] L. Hua, R. Zhou, D. Thirumalai, B.J. Berne, Urea denaturation by stronger dispersion interactions with proteins than water implies a 2-stage unfolding, Proc. Natl. Acad. Sci. U. S. A. 105 (2008) 16928–16933.
[8] W.K. Lim, J. Rösgen, S.W. Englander, Urea, but not guanidinium, destabilizes proteins by forming hydrogen bonds to the peptide group, Proc. Natl. Acad. Sci. U. S. A. 106 (2009) 2595–2600.
[9] D.R. Canchi, A.E. García, Backbone and side-chain contributions in protein denaturation by urea, Biophys. J. 100 (2011) 1526–1533.
[10] M. Gao, Z.S. She, R. Zhou, Key residues that play a critical role in urea-induced lysozyme unfolding, J. Phys. Chem. B 114 (2010) 15687–15693.

[11] I. Eberini, A. Emerson, C. Sensi, L. Ragona, P. Ricchiuto, A. Pedretti, E. Gianazza, A. Tramontano, Simulation of urea-induced protein unfolding: a lesson from bovine beta-lactoglobulin, J. Mol. Graph. Model. 30 (2011) 24–30.
[12] M. Auton, D.W. Bolen, J. Rösgen, Structural thermodynamics of protein preferential solvation: osmolyte solvation of proteins, amino acids, and peptides, Proteins 73 (2008) 802–813.
[13] M. Auton, J. Rösgen, M. Sinev, L.M. Holthauzen, D.W. Bolen, Osmolyte effects on protein stability and solubility: a balancing act between backbone and side-chains, Biophys. Chem. 159 (2011) 90–99.
[14] M. Candotti, S. Esteban-Martín, X. Salvatella, M. Orozco, Toward an atomistic description of the urea-denatured state of proteins, Proc. Natl. Acad. Sci. U. S. A. 110 (2013) 5933–5938.
[15] P.H. Yancey, M.E. Clark, S.C. Hand, R.D. Bowlus, G.N. Somero, Living with water stress: evolution of osmolyte systems, Science 217 (1982) 1214–1222.
[16] D.R. Canchi, P. Jayasimha, D.C. Rau, G.I. Makhatadze, A.E. Garcia, Molecular mechanism for the preferential exclusion of TMAO from protein surfaces, J. Phys. Chem. B 116 (2012) 12095–12104.
[17] S.S. Cho, G. Reddy, J.E. Straub, D. Thirumalai, Entropic stabilization of proteins by TMAO, J. Phys. Chem. B 115 (2011) 13401–13407.
[18] C.Y. Hu, G.C. Lynch, H. Kokubo, B.M. Pettitt, Trimethylamine N-oxide influence on the backbone of proteins: an oligoglycine model, Proteins 78 (2010) 695–704.
[19] J. Mondal, G. Stirnemann, B.J. Berne, When does trimethylamine N-oxide fold a polymer chain and urea unfold it? J. Phys. Chem. B 117 (2013) 8723–8732.
[20] P. Bruździak, A. Panuszko, J. Stangret, Influence of osmolytes on protein and water structure: a step to understanding the mechanism of protein stabilization, J. Phys. Chem. B 117 (2013) 11502–11508.
[21] H. Wei, Y. Fan, Y.Q. Gao, Effects of urea, tetramethyl urea, and trimethylamine N-oxide on aqueous solution structure and solvation of protein backbones: a molecular dynamics simulation study, J. Phys. Chem. B 114 (2010) 557–568.
[22] B.J. Bennion, V. Daggett, Counteraction of urea-induced protein denaturation by trimethylamine N-oxide: a chemical chaperone at atomic resolution, Proc. Natl. Acad. Sci. U. S. A. 101 (2004) 6433–6438.
[23] A.C. Ferreon, M.M. Moosa, Y. Gambin, A.A. Deniz, Counteracting chemical chaperone effects on the single-molecule alpha-synuclein structural landscape, Proc. Natl. Acad. Sci. U. S. A. 109 (2012) 17826–17831.
[24] V. Doan-Nguyen, J.P. Loria, The effects of cosolutes on protein dynamics: the reversal of denaturant-induced protein fluctuations by trimethylamine N-oxide, Protein Sci. 16 (2007) 20–29.
[25] K.A. Cuellar, K.L. Munroe, D.H. Magers, N.I. Hammer, Noncovalent interactions in microsolvated networks of trimethylamine N-oxide, J. Phys. Chem. B 118 (2014) 449–459.
[26] B.J. Bennion, M.L. DeMarco, V. Daggett, Preventing misfolding of the prion protein by trimethylamine N-oxide, Biochemistry 43 (2004) 12955–12963.
[27] D. Wu, A.P. Minton, Quantitative characterization of the compensating effects of trimethylamine-N-oxide and guanidine hydrochloride on the dissociation of human cyanmethmoglobin, J. Phys. Chem. B 117 (2013) 9395–9399.
[28] R. Singh, I. Haque, F. Ahmad, Counteracting osmolyte trimethylamine N-oxide destabilizes proteins at pH below its pKa. Measurements of thermodynamic parameters of proteins in the presence and absence of trimethylamine N-oxide, J. Biol. Chem. 280 (2005) 11035–11042.
[29] T.R. Silvers, J.K. Myers, Osmolyte effects on the self-association of concanavalin A: testing theoretical models, Biochemistry 52 (2013) 9367–9374.
[30] A. Mukherjee, M.K. Santra, T.K. Beuria, D. Panda, A natural osmolyte trimethylamine N-oxide promotes assembly and bundling of the bacterial cell division protein, FtsZ and counteracts the denaturing effects of urea, FEBS J. 272 (2005) 2760–2772.
[31] R. Kumemoto, K. Yusa, T. Shibayama, K. Hatori, Trimethylamine N-oxide suppresses the activity of the actomyosin motor, Biochim. Biophys. Acta 1820 (2012) 1597–1604.
[32] P.H. Yancey, M.E. Gerringer, J.C. Drazen, A.A. Rowden, A. Jamieson, Marine fish may be biochemically constrained from inhabiting the deepest ocean depths, Proc. Natl. Acad. Sci. U. S. A. 111 (2014) 4461–4465.
[33] J.A. Spudich, S. Watt, The regulation of rabbit skeletal muscle contraction. I. Biochemical studies of the interaction of the tropomyosin–troponin complex with actin and the proteolytic fragments of myosin, J. Biol. Chem. 246 (1971) 4866–4871.
[34] E. Andrianantoandro, L. Blanchoin, D. Sept, J.A. McCammon, T.D. Pollard, Kinetic mechanism of end-to-end annealing of actin filaments, J. Mol. Biol. 312 (2001) 721–730.
[35] T. Kouyama, K. Mihashi, Fluorimetry study of N-(1-pyrenyl)iodoacetamide-labelled F-actin. Local structural change of actin protomer both on polymerization and on binding of heavy meromyosin, Eur. J. Biochem. 114 (1981) 33–38.
[36] S. Ishiwata, J. Tadashige, I. Masui, T. Nishizaka, K. Kinosita Jr., Microscopic analysis of polymerization and fragmentation of individual actin filaments, Results Probl. Cell Differ. 32 (2001) 79–94.
[37] R.L. Meeusen, W.Z. Cande, N-ethylmaleimide-modified heavy meromyosin. A probe for actomyosin interactions, J. Cell Biol. 82 (1979) 57–65.
[38] R. Kumemoto, Y. Hosogoe, N. Nomura, K. Hatori, Effects of urea and guanidine hydrochloride on the sliding movement of actin filaments with ATP hydrolysis by myosin molecules, J. Biochem. 149 (2011) 713–720.
[39] A. Narita, S. Takeda, A. Yamashita, Y. Maéda, Structural basis of actin filament capping at the barbed-end: a cryo-electron microscopy study, EMBO J. 25 (2006) 5626–5633.
[40] V.E. Galkin, A. Orlova, G.F. Schröder, E.H. Egelman, Structural polymorphism in F-actin, Nat. Struct. Mol. Biol. 17 (2010) 1318–1323.
[41] T.Y. Lin, S.N. Timasheff, Why do some organisms use a urea–methylamine mixture as osmolyte? Thermodynamic compensation of urea and trimethylamine N-oxide interactions with protein, Biochemistry 33 (1994) 12695–12701.